Volume 9, Issue 3, 2019, 3956 - 3962 ISSN 2069-5837

Biointerface Research in Applied Chemistry

www.BiointerfaceResearch.com

https://doi.org/10.33263/BRIAC93.956962

Original Research Article Open Access Journal

Received: 11.05.2019 / Revised: 05.06.2019 / Accepted: 09.06.2019 / Published on-line: 15.06.2019

Molecular vibration of dopamine neurotransmitter: a relation between its normal modes and harmonic notes

Majid Monajjemi [1]

[1]Department of chemical engineering, Central Tehran Branch, Islamic Azad University, Tehran, Iran

*corresponding author e-mail address: ***Maj.monajjemi@iauctb.ac.ir***

ABSTRACT

Dopamine (3, 4-dihydroxyphenethylamine) is an important compound in the human brain for sending signals to other nerve cells. Dopamine plays major roles in controlling, motivation, arousal, reinforcement, and reward in the brain. Lactation, sexual gratification, and nausea are also results of dopamine pathways. In this study the normal modes analysis of dopamine has been exhibited for understanding their relation between those dopamine structure and harmonic notes. This work demonstrated details of the musical conversion of molecular vibrational based on normal modes analysis of dopamine. The normal modes can be mapped to a spectrum in the audible frequencies ranges, and it can also be mapped to musically useful parameters.

Keywords: *dopamine; normal modes ; harmonic notes.*

1. INTRODUCTION

In the past decades, several attempts have been done for converting the molecular specifics to acoustic and musical behavior. Axen and coworkers in 1996 used a pattern of acoustic conversion due to sonic phenomenon at time coordinates dependent on coordinates of cells [1]. Moreover, nucleic acids linkages of DNA have been converted into sonic musical notes via using a simple coding of DNA bases [2- 5]. In another work, a method illustrated through acoustically converting mass-current oscillations based on the coherent quantum oscillations among the Helium atoms [6]. Based on converting of some molecular specifics such as frequency, amplitude and duration into sound dimensions the field of Sonification has been investigated by Albers 1994, Walker and Kramer 1996 [7, 8]. Although this method is applied for several other physical phenomena by Lunney and Foner, it has been reclaimed with analytical chemistry applications by Yeung and Frysinger in field of Sonification [9-12]. Electromagnetic ray's Sonification (such as infrared electromagnetic) is also a wonderful origin of musical acoustic which can be exhibited via spectral elements of light emitted [12, 13]. Based on base absorption band in DNA a vertical line corresponds to the central frequency of the band has been assigned, while the transposition of this frequency into the acoustic range produces a micro-tonality characteristic of the specific base. With this phenomenon a musical scales related to the DNA bases has been assigned and converted by Alexander, Lunney and Morrison [9-17]. Although the lines were subsequently depend to the notes of the chromatic scales, the data of an entire infrared spectrum being mapped into several octaves. In 1992, McMillan and coworkers [18] applied a neural network for the musical conversion of IR spectrum which the sound was applied for playing the acoustic foundation. In whether scientific and musical objectives necessitate different approaches to Sonification, or whether the same mapping can sometimes be useful for both. Non-scientist musicians may not understand that molecules oscillate and play music under various conditions. In other words due to a very fast vibrate of the atoms in molecules that are orders of a large magnitude faster than acoustic vibrations cannot be possible to hear these frequencies physically. But, it is wondering how the vibrations would sound if mapped into the acoustic region. This perspective is become more amazing by the fact which each kind of molecules even each chemical reaction has a specific spectrum in a wide region. In any modeling of molecular properties towards musical Sonification any vibrations might be matched to the melodies, rhythms, pitch or duration of acoustic. This work demonstrated details of the musical conversion of molecular vibrational based on normal modes analysis. The normal modes can be mapped to a spectrum in the audible frequencies ranges, and it can also be mapped to musically useful parameters. In this study, a piece of music is considered to be a combination of elementary normal modes and depending on the time scale, the nature of the musical parameter, and the implementation, may be discrete or continuous including short or long durations. In the brain, dopamine (scheme 1) functions as an important neurotransmitter compounds released by nerve cells which are known as neurons for sending signals to adjacent nerve cells. Human brains have various pathways for distinct dopamine, for example one of which has a main role in the motivational components of reward-motivated behavior which increases the level of dopamine in the brain [19], and many addictive drugs increase dopamine release or block its reuptake into neurons following release. Other brain's dopamine pathway is consisting of motor control and for releasing of several hormones and this pathway of dopamine system is neuron- modulatory. Although dopamine is often known as the main chemical of pleasure, the current belief in pharmacologist is that dopamine confers motivational salience [20-23]. Dopamine signals the perceived motivational preferences such as musical notes of an outcome that in turn propels the organism's behavior toward that

outcome [23]. Various diseases of the nervous are associated with invalidism of the dopamine system such as Parkinson's disease that is caused by a loss of dopamine-secreting neurons. There is strong witness that schizophrenia involves altered levels of dopamine activities, therefore dopamine as antipsychotic drug can be used for treating this kind disease.

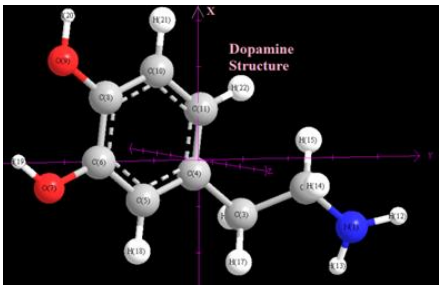

Scheme 1. Dopamine optimized structure.

1.1. Normal modes

In the classical movement of various vibrations, the normal modes are defined as a simple harmonic oscillator including; symmetric stretching, asymmetric stretching bending and improper, The total rules based on normal modes are suitable for musical Sonification of any vibrations which matched to the melodies, rhythms, pitch or duration of acoustic. The basic principles are abstracted as; (1) acts like a simple harmonic oscillator, (2) is a concerted motion of many atoms, (3) the center of mass doesn't move, (4) all atoms pass through their equilibrium positions at the same time and (5) Normal modes are independent without any interaction and are estimated using Newton's rule of motion. $\frac{d^2X}{dt^2} = -4\pi^2\vartheta^2X$ And m. $\frac{d^2X}{dt^2} = -kX \rightarrow -4\pi^2\vartheta^2mX = -kX$ is the basis for the classical calculation of the normal modes of a molecule. Based on Wilson method [FG-λI]=0, F is a Matrix of force constants due to potential energies and G is a matrix involves masses and certain spatial relationships of the atoms due to kinetic energies. "I" is a unit matrix and λ is related to the frequency$\lambda = 4\pi^2\vartheta^2C^2$. As for instance for H_2O in C_{2v} character table the Γ_{3N} consists of E=9, C_2=-1, $\sigma_v(xz) = 3$ and $\sigma_v(yz) = 1$ which can be reduced to $\Gamma_{3N} = 3A_1+A_2+3B_1+2B_2$ and $A_1+A_2+2B_1+2B_2$ are belong to translation and rotation accounts, while $2A_1+ B_1$ belongs to the vibrational modes. Displacements of the internal coordinates including O-H (Δd_1 and Δd_2) distances and HOH angle ($\Delta\theta$) are bases for the irreducible representation (Δd_1, Δd_2) = $A_1+ B_1$ and $\Delta\theta = A_1$. Applying projection operators to only one of the member of Δd_1 or Δd_2 yields: $\hat{p}^{A_1}\ \Delta d_1 = \{(1)\hat{E} +(1)\hat{C}_2 +(1)\ \hat{\sigma}_v(xz) +(1)\ \hat{\sigma}_v(yz)\}\Delta d_1 = \Delta d_1 + \Delta d_2$ and $\hat{p}^{B_1}\ \Delta d_1 = \Delta d_1 - \Delta d_2$. Consequently symmetry coordinates for vibrations are $A_1 = \{S_1 = \Delta\theta$ and $S_2 = \frac{1}{\sqrt{2}}(\Delta d_1 + \Delta d_2)\}$ and $B_1 = \{S_3 = \frac{1}{\sqrt{2}}(\Delta d_1 - \Delta d_2)\}$ and $\frac{1}{\sqrt{2}}$ is the normalized factor to constitute an orthogonal set ($\Delta d_i \Delta d_j = \delta_{ij}$).

The potential energies can be written as $2V = \sum_{i,k} f_{ik}\, s_i s_k$ $(f_{ik} = force\ constants)$ **(1)**, therefore for H_2O there are three internal coordinates and hence nine force constants including

$\boldsymbol{Matrix}$:	$\Delta\mathbf{d_1}$	$\Delta\mathbf{d_2}$	$\Delta\boldsymbol{\theta}$
$\Delta\mathbf{d_1}$	f_d	f_{dd}	$f_{d\theta}$
$\Delta\mathbf{d_2}$	f_{dd}	f_d	$f_{d\theta}$
$\Delta\boldsymbol{\theta}$	$f_{d\theta}$	$f_{d\theta}$	f_θ

where the force constants for (O-H) stretching, (HOH)bending and interaction of one bond stretch to other bond stretch or angle bending are f_d , f_θ , f_{dd} and $f_{d\theta}$ respectively. Therefore the equation (1) can be written as: $2V = f_d(\Delta d_1)^2 + f_d(\Delta d_2)^2 + f_\theta(\Delta\theta)^2 + 2f_{dd}(\Delta d_1 \Delta d_2) + 2f_{d\theta}(\Delta d_1 \Delta\theta) + 2f_{d\theta}(\Delta d_2 \Delta\theta) = \sum_{i,j} F_{ij}\, s_i s_j$

Here the F_{ij} are force constants described by symmetry coordinates of s_i and s_j which provides the easiest routs due to secular equations as 2v=$s'fs$ or 2V=$S'FS$ and it is also to find the relationship between internal coordinates and symmetry coordinates as: S=Us which U Matrix is defined as

$\boldsymbol{UMatrix}$:	$\Delta\mathbf{d_1}$	$\Delta\mathbf{d_2}$	$\Delta\boldsymbol{\theta}$
$\mathbf{s_1}$	0	0	1
$\mathbf{s_2}$	$\frac{1}{\sqrt{2}}$	$\frac{1}{\sqrt{2}}$	0
$\mathbf{s_3}$	$\frac{1}{\sqrt{2}}$	$-\frac{1}{\sqrt{2}}$	0

U' is the invers matrix of U therefore s=$U^{-1}S = U'S$ and $s' = (U'S)' = S'U$ and also it can be easily proved that $UfU' = F$ and by transforming f matrix into F the F Matrix is :

$$\begin{matrix} f_\theta & \sqrt{2}f_{d\theta} & 0 \\ \sqrt{2}f_{d\theta} & f_d + f_{dd} & 0 \\ 0 & 0 & f_d - f_{dd} \end{matrix}$$

The G Matrix can also be calculated from $UgU' = G$

For finding a function of Eigen-vectors converting as a specific irreducible representation, the projection operator might be used in the related group theories and character tables. "F" is defined as an arbitrary function which can be expanded into various irreducible representations $F = \sum_\alpha \sum_n c_\alpha^n\, \xi_\alpha^n$ where α denotes the irreducible representation andc_α^n, $\xi_\alpha^n$are the coefficients of the expansion and functions transforming according to the representation α, respectively. Therefore the projection operators "$\hat{P}$" presented as: $\hat{p}^\beta_{l(n)} = \frac{d_\beta}{g}\sum_G D^\beta_{l(n)}\,(G*)(G)$. In this equation d_β is degeneracy of irreducible representation of β and g is the symmetry order of group and G is the symmetrical operators operations for each l(n) element of $D(\beta)$ character table.

1.2. Projection Operators

From a given irreducible presentation, the functions can be produced along the irreducible presentation. In the orthonormal set *L(i)* of the functions including φ_1^i , φ_2^i , φ_3^i, … φ_L^iwhich is applied for forming the i_{th} irreducible representation of a group by order *h*, for the operators, $\hat{\boldsymbol{R}}$, which defined as $\hat{\boldsymbol{R}}\varphi_t^i = \sum_s \varphi_s^i\, \Gamma(\mathrm{R})^i_{st}$ (1), the multiply of this equation by $[\Gamma(R)^i_{s't'}]^*$ and a summation over the symmetrical function it can be written as : $\sum_R[\Gamma(R)^i_{s't'}]^*\hat{\boldsymbol{R}}\varphi_t^i = \sum_R\sum_S \Gamma\varphi_s^i\,\Gamma(\mathrm{R})^i_{st}\Gamma(R)^i_{s't'}]^*$ (2) Considering are functions independent from *R*, the right side of the equation can be rewritten as: $\sum_s \varphi_s^i \sum_R[\,\Gamma(\mathrm{R})^i_{st}\Gamma(R)^i_{s't'}]^*$. So we have a series of L (i) terms with production of φ_s^i and coefficient of α . These coefficients are obey of orthogonally function: $\sum_R[\Gamma(\mathrm{R})^i_{st}\Gamma(R)^i_{s't'}]^* = (\frac{h}{L_iL_j})^{1/2}\delta_{ij}\delta_{ss'}\delta_{tt'}$ (3) via using the equation (3) the equation (2) will be simplified as follows: $\sum_R[\Gamma(R)^i_{s't'}]^*\ \hat{\boldsymbol{R}}\varphi_t^i = (\frac{h}{L_j})\varphi_{is'}\delta_{ij}\delta_{tt'}$ (4) let us define the projection operator as follows $\hat{P}^j_{s't'} = \frac{L_j}{h}\sum_R[\,\Gamma(\mathrm{R})^i_{st}\Gamma(R)^i_{s't'}]^*\hat{\boldsymbol{R}}$

(5) which yields $\hat{P}^{j}_{s't'}\varphi^{i}_{t} = \varphi_{is'}\delta_{ij}\delta_{tt'}$ (6). The application of the projection operator is projecting function φ^{i}_{t} from any function φ^{i}_{t}. In other words $\hat{P}^{j}_{t''t'}\varphi^{i}_{t} = = \varphi_{t'}\delta_{ij}\delta_{tt'}$ (7). Through using projection operator linear combination of normal modes can be calculated. This linear combination consists of normal mode combinations which matched with melodies, rhythms, pitch or duration of acoustic.

2. MATERIALS AND METHODS

2.1. Wilson methods on dopamine.

In this work the Urey-Bradley force field has been applied and the calculation of normal mode frequencies have been done according to GF Wilson matrix. By this method F Matrix for dopamine has been calculated via $UfU' = F$ transformation and G matrix or inverse kinetic energy matrix for dopamine has been estimated by the equation as follows: $G_{KL} = \sum_{i=1}^{66} B_{ki}\, B_{il}/m_i (k, l = 1, \ldots 3n - 6)$ where m_i is the mass of the i[th] atom. The kinetic energy is given by: $R'GR = 2T$ and $R'FR = 2V$ which R' is transposing of R. The secular equation can be written as [FG- λ I] =0 where the frequency $\lambda = 4\pi^2\vartheta^2C^2$ and the normal coordinate Q is related to the internal coordinate R with the equation R=LQ. And normal mode Q_k is described through the elements of the eigenvector L_k belonging toλ_k. The potential energy distribution helps for finding any coupling of normal modes which can be estimated with projection operator. Potential energy of K[th] normal modes associating with i[th] internal coordinates can be written as:$PE_i^k = \frac{L_{ik}^2 F_{ik}}{\lambda_k}$ Dopamine has 22 atoms or 3N-6=60 modes and the frequencies of these normal modes have been calculated with Wilson GF matrixes. Each assignment can be exhibited based on PED, line intensity and its group theory. Refined force constants and internal coordinate are listed in Table 1.

Table 1. Internal coordinates of dopamine for 60 normal modes.

No	Internal coordinate	No	Internal coordinate	No	Internal coordinate
1	$\vartheta(C_8O_9)$	21	$\vartheta\ (O_9H_{20})$	41	$\vartheta[0.5(\mathbf{7+8})]$
2	$\vartheta(C_6O_7)$	22	$\vartheta\ (O_7H_{19})$	42	$\vartheta[0.5(\mathbf{12+13})]$
3	$\vartheta(C_4C_5)$	23	$\emptyset(C_{10}C_{11}C_4)$	43	$\vartheta[0.5(\mathbf{12-13})]$
4	$\vartheta(C_5C_6)$	24	$\emptyset(C_{11}C_4C_5)$	44	$\vartheta[0.5(\mathbf{21+22})]$
5	$\vartheta(C_6C_8)$	25	$\emptyset(C_4C_5C_6)$	45	$\vartheta[0.5(\mathbf{21-22})]$
6	$\vartheta(C_8C_{10})$	26	$\emptyset(C_5C_6C_8)$	46	$\emptyset[0.5(\mathbf{23+24})]$
7	$\vartheta(C_{10}C_{11})$	27	$\emptyset(C_6C_8C_{10})$	47	$\emptyset[0.5(\mathbf{24+25})]$
8	$\vartheta(C_{11}C_4)$	28	$\emptyset(O_9C_8C_6)$	48	$\emptyset[0.5(\mathbf{25+26})]$
9	$\vartheta(C_4C_3)$	29	$\emptyset(O_9C_8C_{10})$	49	$\emptyset[0.5(\mathbf{26+27})]$
10	$\vartheta(C_3C_2)$	30	$\emptyset(O_7C_6C_8)$	50	$\emptyset[0.5(\mathbf{28+29})]$
11	$\vartheta(C_2N_1)$	31	$\emptyset(O_7C_6C_5)$	51	$\emptyset[0.5(\mathbf{28-29})]$
12	$\vartheta(N_1H_{12})$	32	$\emptyset(C_{11}C_4C_3)$	52	$\emptyset[0.5(\mathbf{30+31})]$
13	$\vartheta(N_1H_{13})$	33	$\emptyset(C_5C_4C_3)$	53	$\emptyset[0.5(\mathbf{30-31})]$
14	$\vartheta(C_2H_{14})$	34	$\emptyset(C_4C_3C_2)$	54	$\emptyset[0.5(\mathbf{32+33})]$
15	$\vartheta(C_2H_{15})$	35	$\emptyset(C_3C_2N_1)$	55	$\emptyset[0.5(\mathbf{33+34})]$
16	$\vartheta(C_3H_{16})$	36	$\vartheta[0.5(\mathbf{1+2})]$	56	$\emptyset[0.5(\mathbf{34+35})]$
17	$\vartheta(C_3H_{17})$	37	$\vartheta[0.5(\mathbf{2+3})]$	57	$\emptyset[0.5(\mathbf{14+15})]$
18	$\vartheta(C_{11}H_{22})$	38	$\vartheta[0.5(\mathbf{3+4})]$	58	$\emptyset[0.5(\mathbf{14-15})]$
19	$\vartheta(C_{10}H_{21})$	39	$\vartheta[0.5(\mathbf{5+6})]$	59	$\emptyset[0.5(\mathbf{16+17})]$
20	$\vartheta(C_5H_{18})$	40	$\vartheta[0.5(\mathbf{6+7})]$	60	$\emptyset[0.5(\mathbf{16-17})]$

2.2. Description of method.

Some of the types of wave function and frequencies as normal modes are listed in table 2 and Fig.1, which can be investigated for any waveforms based on inverse Fourier transforms of vibrational spectra. This spectrum of dopamine is easily transposed down into the audible frequencies area, and its inverse Fourier transform can be taken for yielding a time -domain wave form. A transposition of about 60 notes in around 8 octaves (Table 3 &4) from normal modes yields the spectrum down to the musically useful ranges. (The frequency ratios corresponding to these octaves are approximately 3×10^{10}) (Speed of light cm/second). This procedure converts a vibrational perspective into the acoustic standpoint, or substitution of vibrational into the acoustic region. The spectrum can be converted such a molecular sound via computer software. In another methodology based on inverse Fourier transform of the molecular vibrational, the data of the spectrum will be converted to standard sound frequencies or acoustic notes. It is notable, the resulting wave shape might be present any time-varying musical data. The transposition frequencies for dropping the molecular vibrational waves into the lower-frequencies spectrum yield musical note forms that are important for controlling rhythm and also pitch or timbre. Based on our previous theoretical work and basic of molecular simulation, this work we has been simulated for any further resulting and discussing [24-54].

Table 2. Number of normal modes (No.), Degeneracy (D), Frequency (F) and Intensity (I) of 60 normal modes, Hyper-Chem calculating.

No	D	F	I	No	D	F	I
1	1	20.29	0.077	31	1	608.83	2.025
2	1	32.6	0.185	32	1	643.42	1.931
3	1	47.00	3.263	33	1	662.91	0.882
4	1	57.5	0.638	34	1	685.57	2.476
5	1	70.21	4.531	35	1	713.27	0.200
6	1	89.65	8.005	36	1	734.43	3.927
7	1	129.0	0.201	37	1	759.14	1.184
8	1	149.3	2.963	38	1	816.47	0.330
9	1	160.5	0.528	39	1	827.27	3.450
10	1	188.7	0.206	40	1	933.12	3.075
11	1	213.7	0.612	41	1	1073.0	2.876
12	1	230.5	0.396	42	1	1131.9	0.737
13	1	270.4	0.139	43	1	11.923	2.205
14	1	277.8	1.454	44	1	1226.4	1.373
15	1	286.3	0.253	45	1	1256.8	0.741
16	2	320.3	0.810	46	1	1309.6	2.077
17	2	321.6	1.975	47	1	1319.5	2.177
18	1	352.2	0.370	48	1	1327.1	1.043
19	1	367.4	0.131	49	1	1362.4	10.37
20	1	376.0	0.081	50	1	1373.3	5.423
21	1	386.1	0.073	51	1	1419.8	6.311
22	1	398.2	0.491	52	1	1429.7	10.10
23	1	442.9	0.336	53	1	1492.3	2.901
24	2	454.3	1.360	54	1	1550.4	15.55
25	2	454.9	1.536	55	1	1573.5	32.60
26	1	465.3	2.724	56	1	1648.5	0.064
27	1	498.5	0.070	57	1	1698.6	13.05
28	1	518.5	1.827	58	1	1756.6	127.7
29	1	547.1	2.460	59	1	1790.2	15.62
30	1	575.9	1.448	60	1	1794.2	17.79

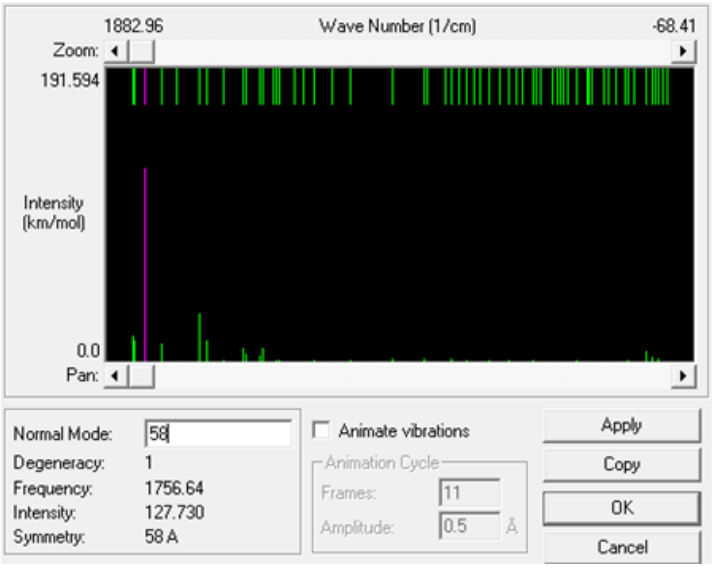

Figure 1. The normal modes analysis of dopamine.

Table 3. Harmonic frequencies (**F**, cm^{-1}), Red Mass (**R**), force constant (**K,** m Dyne/A) and IR intensities (**I** , KM $Mole^{-1}$), for Dopamine with B3LYP/6-31g* method.

No	F	R	K	I	No	F	R	K	I
1	32.6	2.8	0.02	3.7	31	1166.0	1.3	1.0	3.03
2	79.8	4.96	0.02	0.98	32	1178.3	1.5	1.2	11.5
3	93.4	2.26	0.01	5.4	33	1194.3	1.4	1.2	88.2
4	181.3	4.34	0.08	24.9	34	1228.2	1.4	1.3	40.9
5	204.7	1.15	0.03	133.	35	1272.4	1.4	1.4	8.97
6	253.5	1.32	0.05	47.9	36	1303.7	1.9	1.9	37.2
7	264.2	3.22	0.13	2.48	37	1325.6	2.7	2.8	131.
8	297.2	3.34	0.17	2.81	38	1335.8	1.4	1.4	35.0
9	314.1	4.04	0.23	4.09	39	1366.9	1.4	1.6	9.39
10	331.2	3.38	0.21	19.0	40	1369.8	1.5	1.6	141.
11	389.7	5.46	0.48	3.05	41	1406.4	3.2	3.7	22.9
12	432.7	1.19	0.13	70.2	42	1437.7	1.4	1.7	18.8
13	460.1	2.67	0.33	5.86	43	1516.9	2.8	3.8	4.84
14	471.3	3.88	0.50	2.75	44	1520.	1.0	1.5	1.40
15	555.7	4.77	0.86	27.4	45	1545.9	1.0	1.5	3.42
16	594.7	5.30	1.10	2.06	46	1566.5	3.3	4.7	153.
17	638.4	4.75	1.14	5.82	47	1661.7	6.4	10.	42.9
18	702.9	5.14	1.49	0.31	48	1681.4	6.2	10.	3.28
19	764.7	4.04	1.39	12.8	49	1695.5	1.0	1.8	24.9
20	792.7	1.63	0.60	8.50	50	2960.1	1.0	5.5	70.9
21	803.9	1.46	0.55	23.2	51	3030.9	1.0	5.8	29.7
22	806.5	2.26	0.86	19.3	52	3070.6	1.0	6.0	28.9
23	881.6	1.39	0.63	13.7	53	3096.3	1.0	6.2	30.0
24	885.2	1.29	0.59	139.	54	3166.4	1.0	6.4	19.8
25	905.6	1.30	0.62	1.27	55	3194.2	1.0	6.6	16.9
26	963.7	2.60	1.42	10.2	56	3198.0	1.0	6.5	3.3
27	985.1	2.59	1.48	7.63	57	3456.6	1.0	7.4	3.5
28	1061.	2.19	1.45	39.5	58	3541.9	1.0	8.0	1.0
29	1099.	2.13	1.51	5.19	59	3717.4	1.0	8.7	82.0
30	1137.	1.92	1.46	93.5	60	3773.6	1.0	8.9	62.0

Table 4. Frequencies for equal-tempered scale A_4=440HZ.

Note	F (HZ)	λ(cm)	Note	F (HZ)	λ(cm)
$\mathbf{C_0}$	16.35	2109.89	$\mathbf{F^{\#}_4/G^{b}_4}$	369.99	93.24
$\mathbf{C^{\#}_0/D^{b}_0}$	17.32	1991.47	G_4	392.00	88.01
$_{\mathbf{0}}$	18.35	1879.69	$\mathbf{G^{\#}_4/A^{b}_4}$	415.30	83.07
$\mathbf{D^{\#}_0/E^{b}_0}$	19.45	1774.20	A_4	440.00	78.41
$\mathbf{E_0}$	20.60	1674.62	$\mathbf{A^{\#}_4/B^{b}_4}$	466.16	74.01
$\mathbf{F_0}$	21.83	1580.63	B_4	493.88	69.85
$\mathbf{F^{\#}_0/G^{b}_0}$	23.12	1491.91	C_5	523.25	65.93
$\mathbf{G_0}$	24.50	1408.18	$\mathbf{C^{\#}_5/D^{b}_5}$	554.37	62.23
$\mathbf{G^{\#}_0/A^{b}_0}$	25.96	1329.14	D_5	587.33	58.74
$\mathbf{A_0}$	27.50	1254.55	$\mathbf{D^{\#}_5/E^{b}_5}$	622.25	55.44
$\mathbf{A^{\#}_0/B^{b}_0}$	29.14	1184.13	E_5	659.25	52.33
$\mathbf{B_0}$	30.87	1117.67	F_5	698.46	49.39
$\mathbf{C_1}$	32.70	1054.94	$\mathbf{F^{\#}_5/G^{b}_5}$	739.99	46.62
$\mathbf{C^{\#}_1/D^{b}_1}$	34.65	995.73	G_5	783.99	44.01
$\mathbf{D_1}$	36.71	939.85	$\mathbf{G^{\#}_5/A^{b}_5}$	830.61	41.54
$\mathbf{D^{\#}_1/E^{b}_1}$	38.89	887.10	A_5	880.00	39.20
$\mathbf{E_1}$	41.20	837.31	$\mathbf{A^{\#}_5/B^{b}_5}$	932.33	37.00
$\mathbf{F_1}$	43.65	790.31	B_5	987.77	34.93
$\mathbf{F^{\#}_1/G^{b}_1}$	46.25	745.96	C_6	1046.50	32.97
$\mathbf{G_1}$	49.00	704.09	$\mathbf{C^{\#}_6/D^{b}_6}$	1108.73	31.12
$\mathbf{G^{\#}_1/A^{b}_1}$	51.91	664.57	D_6	1174.66	29.37
$\mathbf{A_1}$	55.00	627.27	$\mathbf{D^{\#}_6/E^{b}_6}$	1244.51	27.72
$\mathbf{A^{\#}_1/B^{b}_1}$	58.27	592.07	E_6	1318.51	26.17
$\mathbf{B_1}$	61.74	558.84	F_6	1396.91	24.70
$\mathbf{C_2}$	65.41	527.47	$\mathbf{F^{\#}_6/G^{b}_6}$	1479.98	23.31
$\mathbf{C^{\#}_2/D^{b}_2}$	69.30	497.87	G_6	1567.98	22.00
$\mathbf{D_2}$	73.42	469.92	$\mathbf{G^{\#}_6/A^{b}_6}$	1661.22	20.77
$\mathbf{D^{\#}_2/E^{b}_2}$	77.78	443.55	A_6	1760.00	19.60
$\mathbf{E_2}$	82.41	418.65	$\mathbf{A^{\#}_6/B^{b}_6}$	1864.66	18.50
$\mathbf{F_2}$	87.31	395.16	B_6	1975.53	17.46
$\mathbf{F^{\#}_2/G^{b}_2}$	92.50	372.98	C_7	2093.00	16.48
$\mathbf{G_2}$	98.00	352.04	$\mathbf{C^{\#}_7/D^{b}_7}$	2217.46	15.56
$\mathbf{G^{\#}_2/A^{b}_2}$	103.83	332.29	D_7	2349.32	14.69
$\mathbf{A_2}$	110.00	313.64	$\mathbf{D^{\#}_7/E^{b}_7}$	2489.02	13.86
$\mathbf{A^{\#}_2/B^{b}_2}$	116.54	296.03	E_7	2637.02	13.08
$\mathbf{B_2}$	123.47	279.42	F_7	2793.83	12.35
$\mathbf{C_3}$	130.81	263.74	$\mathbf{F^{\#}_7/G^{b}_7}$	2959.96	11.66
$\mathbf{C^{\#}_3/D^{b}_3}$	138.59	248.93	G_7	3135.96	11.00
$\mathbf{D_3}$	146.83	234.96	$\mathbf{G^{\#}_7/A^{b}_7}$	3322.44	10.38
$\mathbf{D^{\#}_3/E^{b}_3}$	155.56	221.77	A_7	3520.00	9.80
$\mathbf{E_3}$	164.81	209.33	$\mathbf{A^{\#}_7/B^{b}_7}$	3729.31	9.25
$\mathbf{F_3}$	174.61	197.58	B_7	3951.07	8.73
$\mathbf{F^{\#}_3/G^{b}_3}$	185.00	186.49	C_8	4186.01	8.24
$\mathbf{G_3}$	196.00	176.02	$\mathbf{C^{\#}_8/D^{b}_8}$	4434.92	7.78
$\mathbf{G^{\#}_3/A^{b}_3}$	207.65	166.14	D_8	4698.63	7.34
$\mathbf{A_3}$	220.00	156.82	$\mathbf{D^{\#}_8/E^{b}_8}$	4978.03	6.93
$\mathbf{A^{\#}_3/B^{b}_3}$	233.08	148.02	E_8	5274.04	6.54
$\mathbf{B_3}$	246.94	139.71	F_8	5587.65	6.17
$\mathbf{C_4}$	261.63	131.87	$\mathbf{F^{\#}_8/G^{b}_8}$	5919.91	5.83
$\mathbf{C^{\#}_4/D^{b}_4}$	277.18	124.47	G_8	6271.93	5.50
$\mathbf{D_4}$	293.66	117.48	$\mathbf{G^{\#}_8/A^{b}_8}$	6644.88	5.19
$\mathbf{D^{\#}_4/E^{b}_4}$	311.13	110.89	A_8	7040.00	4.90
$\mathbf{E_4}$	329.63	104.66	$\mathbf{A^{\#}_8/B^{b}_8}$	7458.62	4.63
$\mathbf{F_4}$	349.23	98.79	B_8	7902.13	4.37

3. RESULTS

In this study, the possibility controlling of physical properties such as density of states versus normal mode energies (Fig.2) allows the construction of more molecular wave forms, with different time-domain shapes but with the same timbres based on the inverse Fourier transform of a vibrational spectrum. According to the normal modes principles, each mode form is static for a stable and homogeneous musical samples (Tables 4 and 5). Therefore, it is possible to acoustically convert each normal modes of frequency to the relative intensity mapped acoustic notes. A molecular vibrational spectrum is independent of the other physical properties, so it can be separately described versus time and any other conversions of the musical notes spectrum. As a simplified item of that mechanism, it is also feasible for limiting such conversions to the musical's peaks. Such conversions produce a series of simplified normal modes forms. Consequently, each of those normal modes forms can be based either directly on the extracted peaks, or else on their inverse Fourier transforms. If the normal modes of dopamine describe acoustic or molecular sounds, this method is helpful to listen of the specific frequency proportion of the vibrational spectral peaks.

As an instance, each sound of the group corresponds and assigned to a separate key of a musical instrument's keyboard. In other words for the simple item of a series of sinusoidal components, each sound can be considered one note of a normal modes. Once a conversion is produced, the individual acoustic note of the family might be considered as independent notes, which can be composed in any further sequence for producing the large varieties of musical combinations.

Table 5 shows the series notes based on normal modes technique. The dopamine spectrum has been applied for generating group notes of molecular sounds which are played using sine oscillators. Furthermore the rhythms are derived from these sequences and the pitches are played repetitively at a rate symmetrical to the corresponding normal modes frequency. Although the normal modes described in this paper were constructed using theoretical data, other wave based on experimental vibrational ranges could also be used.

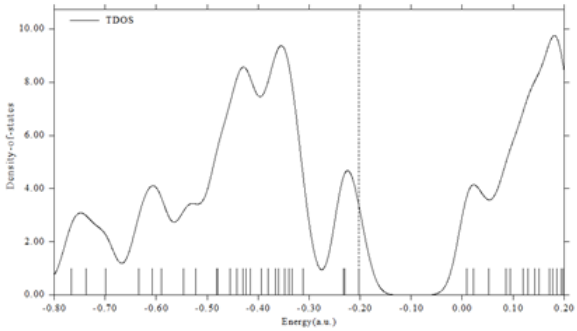

Figure 2. Density of states versus 40 normal modes energies.

Table. 5. Harmonic frequencies (**F**, cm^{-1}), IR intensities (**I** , KM $Mole^{-1}$), and Acoustic frequencies (**A**, HZ) for Dopamine with B3LYP/6-31g* method.

F	I	pitch	A	F	I	pitch	A
32.6	3.7	C_1	32.70	1166.0	3.03	D_6	1174.6
79.8	0.98	D_2	73.42	1178.3	11.5	D_6	1174.6
93.4	5.4	$F^{\#}_2/G^{b}_2$	92.50	1194.3	88.2	D_6	1174.6
181.3	24.9	$F^{\#}_3/G^{b}_3$	185.0	1228.2	40.9	$D^{\#}_6/E^{b}_6$	1244.5
204.7	133.	$G^{\#}_3/A^{b}_3$	207.6	1272.4	8.97	$D^{\#}_6/E^{b}_6$	1244.5
253.5	47.9	B_3	246.9	1303.7	37.2	E_6	1318.5
264.2	2.48	C_4	261.6	1325.6	131.	E_6	1318.5
297.2	2.81	D_4	293.6	1335.8	35.0	E_6	1318.5
314.1	4.09	$D^{\#}_4/E^{b}_4$	311.1	1366.9	9.39	F_6	1396.9
331.2	19.0	E_4	329.6	1369.8	141.	F_6	1396.9
389.7	3.05	G_4	392.0	1406.4	22.9	F_6	1396.9
432.7	70.2	A_4	440.0	1437.7	18.8	$F^{\#}_6/G^{b}_6$	1479.9
460.1	5.86	$A^{\#}_4/B^{b}_4$	466.1	1516.9	4.84	G_6	1567.9
471.3	2.75	B_4	493.8	1520.	1.40	G_6	1567.9
555.7	27.4	$C^{\#}_5/D^{b}_5$	554.3	1545.9	3.42	G_6	1567.9
594.7	2.06	D_5	587.3	1566.5	153.	G_6	1567.9
638.4	5.82	$D^{\#}_5/E^{b}_5$	622.2	1661.7	42.9	$G^{\#}_6/A^{b}_6$	1661.2
702.9	0.31	F_5	698.4	1681.4	3.28	$G^{\#}_6/A^{b}_6$	1661.2
764.7	12.8	$F^{\#}_5/G^{b}_5$	739.9	1695.5	24.9	$G^{\#}_6/A^{b}_6$	1661.2
792.7	8.50	G_5	783.9	2960.1	70.9	$F^{\#}_7/G^{b}_7$	2959.9
803.9	23.2	$G^{\#}_5/A^{b}_5$	830.6	3030.9	29.7	$F^{\#}_7/G^{b}_7$	2959.9
806.5	19.3	$G^{\#}_5/A^{b}_5$	830.6	3070.6	28.9	G_7	3135.9
881.6	13.7	A_5	880.0	3096.3	30.0	G_7	3135.9
885.2	139.	A_5	880.0	3166.4	19.8	G_7	3135.9
905.6	1.27	$A^{\#}_5/B^{b}_5$	932.3	3194.2	16.9	G_7	3135.9
963.7	10.2	$A^{\#}_5/B^{b}_5$	932.3	3198.0	3.3	G_7	3135.9
985.1	7.63	B_5	987.7	3456.6	3.5	A_7	3520.0
1061.	39.5	C_6	1046.	3541.9	1.0	A_7	3520.0
1099.	5.19	C_6	1046.	3717.4	82.0	$A^{\#}_7/B^{b}_7$	3729.3
1137.	93.5	D_6	1174.	3773.6	62.0	$A^{\#}_7/B^{b}_7$	3729.3

4. CONCLUSIONS

The present method explained a sonification ways for normal mode analysis. In other words by this invistegation, the sonification which is application of a non-speech audio to convey information or perceptualize data has been used for normal modes of dopamine. Auditory perception has advantages in temporal, spatial, amplitude, and frequency resolution that open possibilities as an alternative or complement to visualization techniques[55-57].

It can be applied with the following goals: 1. Audio character of a molecular substance, after adopting an efficacious musical coding which is identical for all those analyzing of the same category. For controlling audio real-time of the evolution the chemical sample's properties might be applied for time or analysis zone.

5. REFERENCES

1. Axen, U.; Choi, I. Investigating Geometric Data with Sound. In *Proceedings of the 1996 International Conference on Auditory Display*, 1996.
2. Hayashi, K.; Munakata, N. Basically Musical. *Nature* **1984**, *310*, 96.
3. Ohno, S.; Ohno, M. The All Pervasive Principle of Repetitious Recurrence Governs not only Coding Sequence Construction but also Human Endeavor in Musical Composition. *Immunogenetics* **1986,** *24*, 71-78.
4. Ohno, S. On Periodicities Governing the Construction of Genes and Proteins. *Animal Genetics* **1988**, *19*, 305-316, http://dx.doi.org/10.1111/j.1365-2052.1988.tb00822.x.
5. Munakata, N.; Hayashi, K. Gene Music: Tonal Assignments of Bases and Amino Acids. In *Proceedings of the Visualizing Biological Information Conference, Singapore, World Scientific*, 1995; pp. 72-83.
6. Pereverzev, S.V.; Loshak, A.; Backhaus, S.; Davis, J.C.; Packard, R.E. Quantum Oscillations between Two Weakly Coupled Reservoirs of Superfluid ^{3}He. *Nature* **1997**, *388*, 449-451, https://doi.org/10.1038/41277.
7. Albers, M.C. The Varèse System, Hybrid auditory Interfaces, and Satellite Ground Control: Using Auditory Icons and Sonification in a Complex, Supervisory Control System. In *Proceedings of the International Conference on Auditory Display*, 1994; Volume 3, pp. 13
8. Walker, B.N.; Kramer, G. Mappings and Metaphors in Auditory Displays: An Experimental Assessment. In *Proceedings of the 1996 International Conference on Auditory Display*, 1996.
9. Lunney, D. Adapted Computers as Laboratory Aids for People with Disabilities. *NETWEAVER* **1991**, *7*.
10. Lunney, D. Assistive Technology in the Science Laboratory : A Talking Laboratory Work Station for Visually Impaired Students. *Information Technology and Disability* **1995**, *2*.
11. Lunney, D.; Morrison, R.C. Auditory Presentation of Experimental Data. In *Proceedings of the Society of Photo - Optical Instrumentation Engineers (Extracting Meaning from*

Complex Data: Processing, Display, Interaction), 1990; Bellingham, https://doi.org/10.1117/12.34683.

12. Foner, L.N. Artificial Synesthesia via Sonification: A Wearable Augmented Sensory System. In *Proceedings of the First International Symposium on Wearable Computers*, Los Alamitos, California: IEEE, 1997; Volume 156, pp. 157, https://doi.org/10.1023/A:1019178210975.
13. Yeung, E. S. Pattern Recognition by Audio Representation of Multivariate Analytical Data. *Analytical Chemistry* **1980**, *52*, 1120-1123, https://doi.org/10.1021/ac50057a028.
14. Frysinger, S.P. Applied Research in Auditory Data Representation. In *Proceedings of the Societyof Photo –Optical Instrumentation Engineers (Extracting Meaning from Complex Data: Processing, Display, Interaction)*, Bellingham, Washington: SPIE, 1990; Volume 1259, pp. 130-139, https://doi.org/10.1117/12.19979.
15. Duregon F, Vendramin B, Bullo V, Gobbo S, Cugusi L, Di Blasio A, et al. Effects of exercise on cancer patients suffering chemotherapy-induced peripheral neuropathy undergoing treatment: a systematic review. *Crit Rev Oncol Hematol.* ,**2018**, 121:90–100. doi: 10.1016/j.critrevonc.2017.11.002
16. Reddy, M.A.; Naeem, Z.; Duncan, C.; Robertson F, Herod J, Rennie A, et al. Reduction of severe visual loss and complications following intra-arterial chemotherapy (IAC) for refractory retinoblastoma. *Br J Ophthalmol.*,**2017**, 101:1704–8. doi: 10.1136/bjophthalmol-2017-310294
17. Lodha, S.K.; Wilson, C.M.; Sheehan, R.E. Sounding Uncertainty Visualization. In *Proceedings of IEEE Visualization*. New York, Association of Computing Machinery, 1996; pp. 189-195.
18. Ospina, P.A.; McComb, A.; Wiart, L.E.; Eisenstat, D.D.; McNeely, M.L.; Physical therapy interventions, other than general physical exercise interventions, in children and adolescents before, during and following treatment for cancer. *Cochrane Database Syst Rev.* (2018) CD012924. doi: 10.1002/14651858.CD012924
19. Baliki, M.N.; Mansour, A.; Baria, A.T.; Huang, L.; Berger, S.E.; Fields, H.L.; Apkarian, A.V. Parceling human accumbens into putative core and shell dissociates encoding of values for reward and pain. *The Journal of Neuroscience* **2013,** *33*, 16383–93, https://doi.org/10.1523/JNEUROSCI.1731-13.2013
20. Wenzel, J.M.; Rauscher, N.A.; Cheer, J.F.; Oleson, E.B. A role for phasic dopamine release within the nucleus accumbens in encoding aversion: a review of the neurochemical literature. *ACS Chemical euroscience* **2015**, *6*, 16, https://doi.org/10.1021/cn500255p.
21. Puglisi-Allegra, S.; Ventura, R. Prefrontal/ accumbal catecholamine system processes high motivational salience. *Front. Behav. Neurosci*. **2012**, *6*, 31, https://dx.doi.org/10.3389%2Ffnbeh.2012.00031.
22. Wang, X.; Li, J.; Dong, G.; Yue, J. The endogenous substrates of brain CYP2D. *Eur. J. Pharmacol*. **2014**, *724*, 211–218, https://doi.org/10.1016/j.ejphar.2013.12.025.
23. Seeman, P. Chapter 1: Historical overview: Introduction to the dopamine receptors. In *Neve K (ed.). The Dopamine Receptors*, Springer 2009; pp. 1-22, https://doi.org/10.1007/978-1-60327-333-6_1.
24. Monajjemi, M.; Ghiasi, R.; Ketabi, S.; Pasdar, H.;Mollamin, F. A theoretical study of metal-stabilised rare tautomers stability: N4 metalated cytosine (M=Be2+, Mg2+,Ca2+, Sr2+ and Ba2+) in gas phase and different solvents. *Journal of chemical research* **2004**, *1*, 11-18, https://doi.org/10.3184/030823404323000648.
25. Monajjemi, M.; Ghiasi, R.; Sadjadi, M.A.S. Metal-stabilized rare tautomers: N4 metalated cytosine (M = Li+, Na+, K+, Rb+ and Cs+), theoretical views. *Applied organometallic chemistry* **2003**, *17*, 635-640, https://doi.org/10.1002/aoc.469.
26. Monajjemi, M.; Mahdavian, L.; Mollaamin, F.;Honarparvar, B. Thermodynamic Investigation of EnolKeto Tautomerism for Alcohol Sensors Based on Carbon Nanotubes as Chemical Sensors. *Fullerenes nanotubes and carbon nanostructures* **2010**, *18*, 45-55, https://doi.org/10.1080/ 15363830903291564.
27. Hadad, B.K.; Mollaamin, F; Monajjemi, M. Biophysical chemistry of macrocycles for drug delivery: a theoretical study. *Russian chemical bulletin* **2011**, *60*, 238-241, https://doi.org/10.1007/s11172-011-0039-5.
28. Monajjemi, M.; Honaparvar, B.; Hadad, B.K.; Ilkhani, A.R.; Mollaamin F. Thermo-chemical investigation and NBO analysis of some anxileotic as Nano- drugs. *African journal of pharmacy and pharmacology* **2010**, *4*, 521-529.
29. Becke, A.D.; Edgecombe, K.E. A. simple measure of electron localization in atomic and molecular systems. *The Journal of Chemical Physics* **1990**, *92*, 5397-5403, https://doi.org/10.1063/1.458517.
30. Lu, T.; Chen, F. Multiwfn: A Multifunctional Wavefunction Analyzer. *J. Comp. Chem*. **2012**, *33*, 580-592, https://doi.org/10.1002/jcc.22885.
31. Monajjemi, M.; Naderi, F.; Mollaamin, F.; Khaleghian, M. Drug Design Outlook by Calculation of Second Virial Coefficient as a Nano Study. *Journal of the mexican chemical society* **2012**, *56*, 207-211.
32. Monajjemi, M.; Mohammadian, N.T.S-NICS an Aromaticity Criterion for Nano Molecules. *J. Comput . Theor. Nanosci* **2015**, *12*, 4895-4914**.**
33. Monajjemi, M.; Lee, V.S.; Khaleghian, M.; Honarparvar, B.; Mollaamin, F. Theoretical Description of Electromagnetic Nonbonded Interactions of Radical, Cationic, and Anionic NH2BHNBHNH2 Inside of the B18N18 Nanoring. *J. Phys. Chem C* **2010**, *114*, 15315, http://dx.doi.org/10.1021/jp104274z.
34. Monajjemi, M.; Boggs, J.E.; A New Generation of BnNn Rings as a Supplement to Boron Nitride Tubes and Cages. *J. Phys. Chem. A* **2013**, *117*, 1670-1684, http://dx.doi.org/10.1021/jp312073q.
35. Monajjemi, M. Non bonded interaction between BnNn (stator) and BN B (rotor) systems: A quantum rotation in IR region. *Chemical Physics* **2013**, *425*, 29-45, https://doi.org/10.1016/j.chemphys.2013.07.014.
36. Monajjemi, M.; Robert, W.J.; Boggs, J.E. NMR contour maps as a new parameter of carboxyl's OH groups in amino acids recognition: A reason of tRNA–amino acid conjugation. *Chemical Physics* **2014**, *433*, 1-11, https://doi.org/10.1016/j.chemphys.2014.01.017.
37. Monajjemi, M. Quantum investigation of non-bonded interaction between the B15N15 ring and BH2NBH2 (radical, cation, and anion) systems: a nano molecularmotor. *Struct Chem* **2012,** *23*, 551–580, http://dx.doi.org/10.1007/s11224-011-9895-8.
38. Monajjemi, M. Non-covalent attraction of B2N (2, 0) and repulsion of B2N (+) in the BnNn ring: a quantum rotatory due to an external field. *Theor Chem Acc* **2015**, 1668-9, https://doi.org/10.1007/s00214-015-1668-9.
39. Monajjemi, M. Metal-doped graphene layers composed with boron nitride–graphene as an insulator: a nano-capacitor. *Journal of Molecular Modeling* **2014**, *20*, 2507, https://doi.org/10.1007/s00894-014-2507-y.

40. Ilkhani, A.R.; Monajjemi, M. The pseudo Jahn-Teller effect of puckering in pentatomic unsaturated rings C(4)AE(5), A = N, P, As, E = H, F, Cl. *Computational and theoretical chemistry* **2015**, *1074*, 19-25.
41. Monajjemi M. Graphene/(h-BN)*n*/X-doped raphene as anode material in lithium ion batteries (X = Li, Be, B AND N). *Macedonian Journal of Chemistry and Chemical Engineering* **2017**, *36*, 101–118, http://dx.doi.org/10.20450/mjcce.2017.1134.
42. Monajjemi, M.; Najafpour, J. Charge density discrepancy between NBO and QTAIM in single-wall armchair carbon nanotubes. *Fullerenes Nanotubes and Carbon Nanostructures* **2014**, *22*, 575-594, https://doi.org/10.1080/1536383X.2012.702161.
43. Monajjemi, M. Cell membrane causes the lipid bilayers to behave as variable capacitors: A esonance with self-induction of helical proteins. *Biophysical Chemistry* **2015**, *207*, 114 –127, https://doi.org/10.1016/j.bpc.2015.10.003.
44. Mollaamin, F.; Monajjemi, M. DFT outlook of solvent effect on function of nano bioorganic drugs. *Physics and Chemistry of Liquids* **2012**, *50*, 596-604, https://doi.org/10.1080/00319104.2011.646444.
45. Monajjemi, M.; Chegini, H.; Mollaamin, F.; Farahani, P. Theoretical Studies of Solvent Effect on Normal Mode Analysis and Thermodynamic Properties of Zigzag (5,0) carbon nanotube. *Fullerens Nanotubes carbon and nanostructures* **2011**, *19*, 469-482, https://doi.org/10.1080/1536383X.2010.494783.
46. Monajjemi, M. Study of CD5+ Ions and Deuterated Variants (CHxD(5-x)+): An Artefactual Rotation. *Russian Journal of Physical Chemistry a* **2018,** *92*, 2215-2226.
47. Monajjemi, M.; Baei, M.T.; Mollaamin, F. Quantum mechanics study of hydrogen chemisorptions on nanocluster vanadium surface. *Russian journal of inorganic chemistry* **2008,** *53*, 1430-1437, https://doi.org/10.1134/S0036023608090143.
48. Monajjemi, M. Liquid-phase exfoliation (LPE) of graphite towards graphene: An ab initio study. *Journal of Molecular Liquids* **2017**, *230*, 461–472, https://doi.org/10.1016/j.molliq.2017.01.044.
49. Monajjemi, M.; Mahdavian, L.; Mollaamin, F. Interaction of Na, Mg, Al, Si with carbon nanotube (CNT): NMR and IR study. *Russian Journal of Inorganic Chemistry* **2009,** *54*, 1465-1473, https://doi.org/10.1134/S0036023609090216.
50. Monajjemi, M.; Ahmadianarog, M. Carbon Nanotube as a Deliver for Sulforaphane in Broccoli Vegetable in Point of Nuclear Magnetic Resonance and Natural Bond Orbital Specifications. *Journal of computational and theoretical nanoscience* **2014**, *11*, 1465-1471, http://dx.doi.org/10.1166/jctn.2014.3519.
51. Lee, V.S.; Nimmanpipug, P.; Mollaamin, F.; Kungwan, N.; Thanasanvorakun, S.; Monajjemi, M. Investigation of single wall carbon nanotubes electrical properties and mode analysis: Dielectric effects. *Russian journal of physical chemistry A* **2009**, *83*, 2288-2296, https://doi.org/10.1134/S0036024409130184.
52. Mollaamin, F.; Najafpour, J.; Ghadami, S.; Akrami, M.S.; Monajjemi, M. The Electromagnetic Feature of B15N15Hx (x=0,4, 8, 12, 16, and 20) Nano Rings: Quantum Theory of Atoms in Molecules /NMR Approach. *Journal of computational and theoretical nanoscience* **2014**, *11*, 1290-1298, https://doi.org/10.1166/jctn.2014.3495.
53. Monajjemi, M.; Ahmadianarog, M. Carbon Nanotube as a Deliver for Sulforaphane in Broccoli Vegetable in Point of Nuclear Magnetic Resonance and Natural Bond Orbital Specifications. *Journal of computational and theoretical nanoscience* **2014**, *11*, 1465-1471, https://doi.org/10.1166/jctn.2014.3519.
54. Monajjemi, M.; Mahdavian, L.; Mollaamin, F. Characterization of nanocrystalline silicon germanium film and nanotube in adsorption gas by monte carlo and langevin dynamic simulation. *Bulletin of the chemical society of Ethiopia* **2008**, *22*, 277-286, http://dx.doi.org/10.4314/bcse.v22i2.61299.
55. Kroschinsky, F.; Stölzel, F.; von Bonin, S.; Beutel, G.; Kochanek, M.; Kiehl, M.; New drugs, new toxicities: severe side effects of modern targeted and immunotherapy of cancer and their management. *Critical Care* **2017,** 21, 89, http://dx.doi.org/10.1186/s13054-017-1678-1
56. Marshall, T.F.; Zipp, G.P.; Battaglia, F.; Moss, R.;Bryan, S.;Chemotherapyinduced-peripheral neuropathy, gait and fall risk in older adults following cancer treatment. *J Cancer Res Pract.* **2017**, 4, 134–8. http://dx.doi.org/10.1016/j.jcrpr.2017.03.005
57. Smart, D.; Radiation Toxicity in the central nervous system: mechanisms and strategies for injury reduction. *Semin Radiat Oncol.* **2017**, 27, 332–9, http://dx.doi.org/10.1016/j.semradonc.2017.04.006

6. ACKNOWLEDGEMENTS

The author thanks the Islamic Azad university for providing the software and computer equipment.